Journal of Catalysis 340 (2016) 219–226

Contents lists available at ScienceDirect

Journal of Catalysis

journal homepage: www.elsevier.com/locate/jcat

The use of bimetallics to control the selectivity for the upgrading of lignin-derived oxygenates: Reaction of anisole on Pt and PtZn catalysts

Daming Shi, Lisandra Arroyo-Ramírez, John M. Vohs *

Department of Chemical & Biomolecular Engineering, University of Pennsylvania, Philadelphia, PA 19104-6363, USA

ARTICLE INFO

Article history:
Received 17 March 2016
Revised 20 May 2016
Accepted 22 May 2016
Available online 13 June 2016

Keywords:
Anisole
Lignin
Hydrodeoxygenation (HDO)
TPD
HREELS
Bimetallic

ABSTRACT

The adsorption and reaction of anisole on Pt and PtZn catalysts were investigated using both model single crystal and high surface area supported metal catalysts. Temperature programmed desorption (TPD) and high resolution electron energy loss spectroscopy (HREELS) studies of the interaction of anisole with Pt (1 1 1) demonstrated that there is a strong interaction between the phenyl ring of anisole and the surface, resulting in C—O and C—H bond scission at relatively low temperatures. In contrast, anisole was observed to bond to a Zn-modified Pt(1 1 1) surface primarily via the oxygen at Zn sites or possibly adjacent Pt sites, with the phenyl ring tilted away from the surface. Such bonding configuration facilitated selective C—O bond cleavage producing phenyl groups and methoxide groups with the latter being bonded to the Zn sites. These results suggested that PtZn may be an effective catalyst for hydrodeoxygenation (HDO) of lignin-derived aromatic oxygenates with low activity for ring hydrogenation. This hypothesis was then tested and verified by investigating the reaction of anisole and H_2 over high surface area carbon-supported Pt and PtZn catalysts.

1. Introduction

Lignocellulosic biomass is emerging as an attractive, sustainable carbon feedstock for the production of fuels and chemicals [1–3]. While in recent years much effort has been focused on catalytic processing of the cellulosic fraction of biomass for this purpose [4–6], the lignin fraction is also a useful resource and provides a feedstock for the production of high-value aromatic compounds [2,7]. The refractory nature of lignin, however, makes its conversion to useful products more challenging than that of cellulose. Depolymerization of lignin is generally achieved via fast pyrolysis which produces a complex liquid mixture containing a range of substituted aromatics [8]. This bio-oil is highly oxygenated and subsequent hydrodeoxygenation (HDO) is usually required.

Conventional metal-sulfide based hydrotreating catalysts (e.g. sulfided CoMo) have been suggested for use in the upgrading and deoxygenation of lignin-derived aromatic oxygenates; unfortunately, they tend to produce less desirable ring saturation products and also rapidly deactivate due to coking [9–12]. Some success has been obtained using group 10 metal catalysts (i.e. Ni, Pd, Pt), but they also promote hydrogenation of the aromatic rings [13,14]. Alloying a group 10 metal with a second more oxyphilic metal (e.g. Fe, Sn, Zn) [15–18], however, has emerged as a promising strategy for producing HDO catalysts that exhibit high selectivity for the production of aromatic hydrocarbons from lignin-derived oxygenates. Multiple studies have shown that alloying Pt or Pd with Sn or Fe weakens the interaction of the aromatic ring with the metal surface, and it has been proposed that this may affect the ring hydrogenation activity by altering the bonding configuration of aromatic oxygenates from one where the ring is lying flat on the surface to one where adsorption occurs primarily via the oxygen functionality [19–21].

Recently our group has undertaken a series of mechanistic studies of the adsorption and reaction of benzaldehyde and other small aldehydes on Pt—Zn model catalysts consisting of a Pt(1 1 1) surface decorated with Zn adatoms [22–24]. Our studies of benzaldehyde on these catalysts provide direct evidence that alloying does indeed alter the bonding configuration of the phenyl ring with the ring tilting away from the surface upon Zn addition. Furthermore, these previous studies show that aldehydes bond to the Zn/Pt (1 1 1) surface via the carbonyl in an η_2-configuration in which the oxygen in the carbonyl is bonded to a Zn site and the carbon is bonded to an adjacent Pt site. This bonding configuration results in a weakening of the C=O bond which helps facilitate its cleavage.

In the work described here we have extended our previous studies of the reactivity of Zn-modified Pt surfaces to include the adsorption and reaction of anisole ($CH_3OC_6H_5$). This molecule

* Corresponding author.
E-mail address: vohs@seas.upenn.edu (J.M. Vohs).

http://dx.doi.org/10.1016/j.jcat.2016.05.020
0021-9517/

was chosen as a model aromatic compound that contains a C—O—C linkage which is commonly found in lignin-derived oxygenates [25–27]. Temperature-programmed desorption (TPD) and high-resolution electron energy loss spectroscopy (HREELS) were used to characterize the pathways and intermediates involved in the reaction of anisole on both Pt(1 1 1) and Zn/Pt(1 1 1) surfaces. Based on the results for the model catalysts we have predicted trends in selectivity for the reaction of anisole on high surface area supported Pt and PtZn catalysts. These predictions were then tested by measuring product selectivity for the reaction of anisole over Pt/C and PtZn/C catalysts under typical HDO reaction conditions. The results from the model and high surface area catalysts together provide useful insight into the active sites in bimetallic HDO catalysts as well as how alloying can be used to limit activity for ring hydrogenation.

2. Experimental

The model catalyst studies in this work were conducted in an ultra-high vacuum (UHV) apparatus described in detail in previous publications [22,28,29]. The system had a background pressure operated at 2×10^{-10} torr and was equipped with a quadruple mass spectrometer (SRS RGA200), an ion sputter gun (PHI electronics) and an HREEL spectrometer (LK Technologies). A Pt(1 1 1) single crystal substrate that was 10 mm in diameter and oriented to within ±0.5° was spot-welded to two tantalum wires that were connected to the UHV sample manipulator. The Pt(1 1 1) surface was cleaned by repeated cycles of 2 kV Ar^+ ion bombardment at 600 K for 40 min, annealing at 1200 K under 2×10^{-8} torr O_2 for 15 min, and annealing at 1200 K in vacuum for 5 min. The sample was heated resistively and cooled to 110 K by conduction from a liquid N_2 reservoir.

Zn deposition on Pt(1 1 1) was obtained by exposing the Pt surface to a beam of Zn atoms produced from an effusive source consisting of a coil of Zn wire (Alfa Aesar, 99.99%) around a resistively heated tungsten filament. A quartz crystal microbalance (QCM) was used to monitor the Zn flux from the source and the total amount of Zn deposited was further quantified by measuring the area of the high-temperature Zn desorption feature in the TPD spectra [22,30]. Detailed characterization of the structure of Zn-modified Pt(1 1 1) surfaces has been reported previously [30]. In that study it was shown that for initial submonolayer amounts of Zn deposited with Pt(1 1 1) sample held at or below room temperature, the Zn diffuses into the surface upon annealing between 600 and 700 K with the equilibrium structure being one where the Zn atoms reside in the second and third layer below the surface. For this structure there are no Zn sites present on the Pt(1 1 1) surface. Since for this study we wanted to investigate how Zn affects reactivity via electronic interactions and its potential role as an active site for HDO, we chose to investigate Pt(1 1 1) surfaces that were decorated with Zn adatoms that were formed by Zn deposition with the Pt(1 1 1) sample below room temperature. Our previous studies have shown that Zn adatoms influence the electronic property of nearby surface Pt atoms in a manner similar to that in the bulk alloy [22].

For the UHV studies the anisole reactant (Sigma-Aldrich, 99.7%) was contained in a glass vial attached to a stainless steel manifold that was connected to the main UHV apparatus via a variable leak valve. A saturation exposure of anisole (0.6 L) was used in both the TPD and HREEL experiments. A heating rate of 3 K/s was used in the TPD experiments and the HREEL spectra were collected using a 4 eV electron beam oriented at 60° with respect to the surface normal. The full width at half-maximum of the elastic peak obtained from the clean surface was typically 40 cm^{-1}. HREEL spectra were collected as a function of sample temperature. For temperatures greater than the dosing temperature the sample was heated at 3 K/s to the indicated temperature and then rapidly quenched to low temperature at which point the spectrum was collected.

Micro flow reactor studies were also carried out to determine the reactivity of carbon supported Pt and PtZn catalysts for the HDO of anisole and to provide comparison data to the model catalyst studies. Pt/C catalysts with 10 wt% Pt were prepared by impregnation of carbon black (Vulcan XC-72R) with a water/ethanol (4:1) solution of tetraammineplatinum (II) nitrate ($Pt(NH_3)_4(NO_3)_2$, 99.99%, Alfa Aesar). The 10 wt% PtZn/C samples were prepared by co-impregnation with water/ethanol (4:1) solution of $Pt(NH_3)_4(NO_3)_2$ and $Zn(NO_3)_2{\cdot}6H_2O$. Prior to reaction studies the catalysts were reduced in flowing 5% H_2/He to 673 K with a heating ramp of 2 K/min, and then to 773 K with heating ramp of 1 K/min at which point it was held for 2 h. PtZn catalysts were prepared with Pt:Zn molar ratios of 1:1 (PtZn/C) and 1:3 ($PtZn_3$/C). Both the PtZn/C and $PtZn_3$/C catalysts had a total metals loading of 10 wt%.

A high-pressure flow reactor that was similar to that described by Luo et al. [31] was used in the reactor studies. The reactor consisted of a 20 cm long, stainless-steel tube (4.6-mm ID) that was heated in a tube furnace. A 1 wt% liquid solution of anisole (Sigma-Aldrich, 99.7%) dissolved in *n*-heptane (Sigma-Aldrich, 99%) was introduced into the reactor by an HPLC pump (Series III, Lab Alliance). The pump was also used to monitor the total pressure which was controlled by a back pressure regulator (KPB series, Swagelok) that was located downstream from the reactor. The pressure was fixed at 27.5 bar for all the experiments performed in this study. Hydrogen (Airgas, UHP grade) contained in a regulated, high-pressure cylinder was delivered to the reactor through 2.44 m of capillary tubing (50.8 μm ID, Valco Instrument, Inc.). The H_2 flow rate was a function of the cylinder outlet pressure and the pressure drop across the capillary tube. For a typical experiment, the liquid flow rate was set as 0.1 ml/min, while the H_2 flow rate was kept constant at 5 ml/min (STP).

For each catalyst test, 0.05 g of the catalyst was packed into the middle portion of the reactor and held in place by glass wool. Prior to rate measurements, each catalyst was pretreated by heating in 27.5 bar of flowing H_2 at 573 K for 30 min. Fresh samples were used for each experiment at a specified reaction condition. The liquid phase reaction products were collected at room temperature and a GC–MS (QP-5000, Shimadzu) was used for identification and quantification of the produces. Product selectivity was quantified using solutions with known concentrations as standards. The reactivity data presented here were obtained 60 min after starting the reaction in order to allow steady state to be obtained.

3. Results and discussion

3.1. Reaction of anisole on Pt(1 1 1)

The initial studies of the adsorption and reaction of anisole were performed for the Zn-free Pt(1 1 1) surface. TPD data collected as a function of coverage were used to determine the dosage required to saturate the surface with anisole, as determined by the appearance of a molecular anisole peak at 185 K corresponding to desorption of adsorbed multilayers. Based on these results, a 0.6 L anisole dose, which gives a coverage slightly more than one monolayer, was chosen for the more detailed TPD studies.

Fig. 1 displays a complete set of TPD data obtained from the Zn-free Pt(1 1 1) surface for the 0.6 L anisole dose. The two low-temperature anisole desorption peaks at 185 and 215 K correspond to physisorbed multilayers and chemisorbed anisole, respectively. The only reaction products detected for this surface were H_2 and

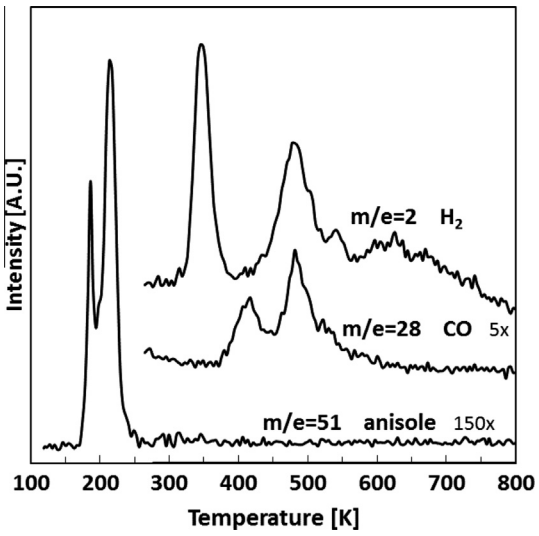

Fig. 1. TPD spectra obtained following exposure of the Pt(1 1 1) surface to 0.6 L of anisole.

CO. Hydrogen was produced in two distinct peaks centered at 350 and 480 K, and a much broader feature that spanned from 530 K to 750 K. The H_2 peak at 350 K is at the same temperature as that reported for recombinative desorption of H atoms on Pt(1 1 1) [32] and therefore indicates that some C—H bond scission in adsorbed anisole has already occurred by this temperature. CO was primarily produced in two peaks centered at 420 and 480 K, with a smaller peak present at 530 K. From the TPD data alone it is not possible to definitively assign these peaks as desorption or reaction limited, although the fact that both CO and H_2 are produced at 480 K suggests that the CO at this temperature is reaction limited.

HREELS was used to provide insight into the identity of adsorbed intermediates formed from anisole on the Pt(1 1 1) surface. HREEL spectra as function of temperature for Pt(1 1 1) dosed with 0.6 L of anisole at 115 K are displayed in Fig. 2. As noted above, spectra corresponding to higher temperatures were obtained by briefly heating the sample to the indicated temperature and then letting it cool back to 115 K, at which point the spectrum was collected. As would be expected, the spectrum obtained at 115 K contains peaks that are characteristic of molecular anisole and can be assigned via comparison with the corresponding IR and Raman spectra [33–35]. Individual peak assignments are given in Table 1.

Heating to 200 K to desorb physisorbed anisole caused only minor changes in the HREEL spectrum including an increase in the intensity of the out-of-plane $\gamma(C—H)_{ring}$ peak at 820 cm^{-1}, diminution in the intensity of the in-plane $\delta(C—H)_{ring}$ peak at 1010 cm^{-1}, and disappearance of the peak at 1250 cm^{-1} which is likely due to both $\nu(C—OMe)$ and in-plane $\nu(C—H)_{ring}$ modes. At such a low temperature it is unlikely that any chemical transformations of the adsorbed anisole have occurred; thus, these intensity changes must be due to the orientation of the chemisorbed anisole relative to the more random orientation for the physisorbed species. In particular, the decrease in the intensities of the peaks for in-plane modes relative to those for out-of-plane modes indicates that the aromatic ring is situated parallel to the surface in the chemisorbed species. This conclusion relies on the fact that an induced image dipole in the metal partially shields vibrational modes which have dipole moments parallel to the surface, thereby decreasing their HREELS cross section. It is also consistent with DFT studies of the interaction of anisole with Pt(1 1 1) reported by Bonalumi et al. [36,37] which showed that the aromatic ring

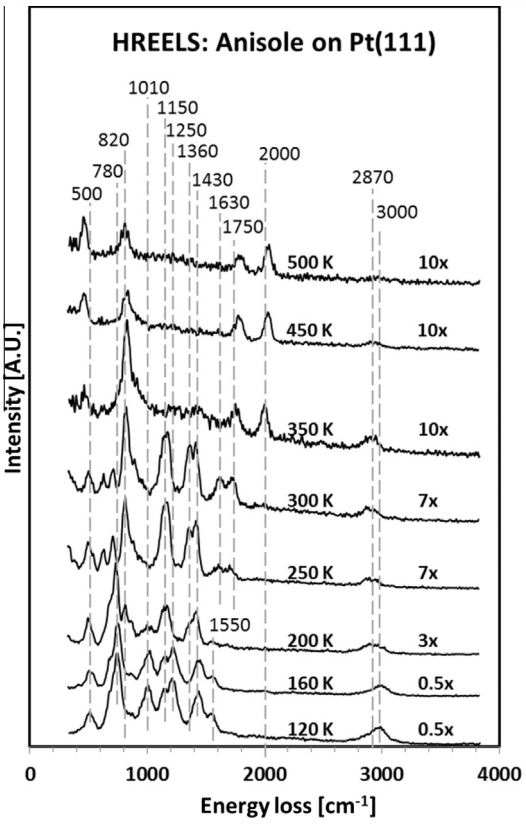

Fig. 2. HREEL spectra as a function of temperature for Pt(1 1 1) dosed with 0.6 L anisole at 115 K.

Table 1
Vibrational mode assignments.

Mode	Frequency (cm^{-1})		
	IR/Raman [33–35]	Pt (1 1 1)	Zn/Pt (1 1 1)
$\gamma(C—C)_{ring}$ (out of plane mode)	509,513	500	500
Ring breathing	785	780	780
$\gamma(C—H)_{ring}$ (out of plane mode)	823,859	820	–
$\gamma(C—H)_{ring}$ (out of plane mode)	878,894	880	–
$\delta(C—H)_{ring}$ (in plane mode)	1022,1029,997	1010	1000
$\nu(O—Me) + b(C—H)_{ring}$ (out of plane mode)	1182,1183	1150	1150
$\nu(C—OMe) + \nu(C—H)_{ring}$ (in plane mode)	1247,1252,1253	1250	1250
$\delta(C—C)_{ring}$ (in plane mode) + $\delta(C—H)_{methyl}$	1453,1436,1468,1422	1430	1440
$\nu(C—C)_{ring}$ (in plane mode)	1588,1513	1550	1560
$\nu(C—H)_{methyl}$	2900	2870	2880
$\nu(C—H)_{ring}$	3004	3000	3000
$\nu(O—H)$	–	–	3500
$\nu(Zn—O)$	–	–	400
$\nu(Pt—C)$	–	470	470

s – symmetric, as – asymmetric, b – bend, ν – stretch, δ – deformation, ρ – rock, γ – wag, χ – scissor.

in anisole adsorbs in the same bridge site in which benzene adsorbs on this surface [38]. In this configuration the $O—CH_3$ group is slightly tilted away from the surface.

Further heating the anisole-dosed Pt(1 1 1) surface to 250 K and then 300 K led to significant changes in the HREEL spectrum. These include a large decrease in the intensity of the ring breathing mode at 780 cm^{-1}, the further emergence of an intense peak at 825 cm^{-1} and smaller peaks at 1630 and 1750 cm^{-1}. Changes were also observed in the C—H stretching region of the spectrum with the

intensity of the $\nu(C—H)_{ring}$ mode decreasing relative to that of the aliphatic $\nu(C—H)$ mode at 2870 cm^{-1}. These signify that reaction or decomposition of the adsorbed anisole has started to occur by 300 K. While it is difficult to unambiguously assign the spectrum at this temperature to specific specie(s), the large decrease in the intensity of the ring breathing mode and the change in the relative intensities of the aromatic and aliphatic $\nu(C—H)$ modes suggests a loss of aromatic character for at least a portion of the adsorbed intermediates.

Even more dramatic changes occurred in the HREEL spectrum obtained upon heating the sample to 350 K. At this temperature the spectrum was dominated by an intense peak at 825 cm^{-1}. Smaller peaks are also apparent at 470, 1750, 2000, and 2870 cm^{-1}, as well as several poorly resolved peaks between 1000 and 1450 cm^{-1}. The peak at 2000 cm^{-1} can be assigned to CO adsorbed in atop sites and indicates that some C—C bond cleavage has started to occur by this temperature. We also assign the peak at 1750 cm^{-1} to adsorbed CO but in bridging sites. While this is an unusually low frequency for bridging CO, previous studies have shown that co-adsorbed electron-donating molecules, such as benzene, can cause a significant decrease in the C—O stretching frequency by increasing the amount of back donation of *d*-electrons from the metal into the π^* anti-bonding orbitals of the adsorbed CO [39,40]. We believe that something similar is happening here. The fact that this peak shifts to 1800 cm^{-1} upon heating to higher temperatures which causes complete decomposition of the anisole reactant is also consistent with this explanation. It is noteworthy that with the exception of these $\nu(CO)$ peaks, the HREEL spectrum at this temperature is nearly identical to that reported by Ihm and White for an oxocyclohexadienyl intermediate (C_6H_6O, 2,5-cyclohexadienone) that is formed by reaction of phenol on Pt(1 1 1) [41]. In that study it was shown that this species bonds to the surface in an η_5-π configuration. To further illustrate this similarity we collected HREEL spectra for a phenol-dosed Pt (1 1 1) surface and the spectrum obtained after heating to 400 K is included in the supplemental information. We, therefore, propose that an oxocyclohexadienyl species is also formed via the reaction of anisole on Pt(1 1 1). The near disappearance of the characteristic aromatic C—H stretch near 3000 cm^{-1} is also consistent with this conclusion.

Formation of an oxocyclohexadienyl intermediate requires cleavage of the $O—CH_3$ bond in anisole and the addition of an H atom to the ring. The $O—CH_3$ bond cleavage would also produce adsorbed methyl groups. Previous studies of the interaction of methyl groups with Pt(1 1 1) show that they are unstable on this surface above 230 K and undergo dehydrogenation to produce adsorbed C and H [42]; thus, the desorption-limited H_2 peak at 350 K in the TPD data in Fig. 1 can be attributed to the H formed by this dehydrogenation reaction. The peak at 470 cm^{-1} in the HREEL spectrum that appears after heating to 350 K can be assigned to a Pt—C stretch of the associated carbon atoms.

Heating the anisole-dosed Pt(1 1 1) sample above 350 K caused the gradual disappearance of the vibrational peaks associated with adsorbed hydrocarbon intermediates with the peaks for adsorbed CO persisting up to 500 K. This result along with the simultaneous H_2 and CO peaks at 480 K in the anisole TPD data (Fig. 1) indicates that the oxocyclohexadienyl intermediate undergoes unselective decomposition near this temperature. This would produce small CH_x fragments that apparently undergo further dehydrogenation at higher temperatures giving rise to the broad H_2 desorption feature between 550 and 750 K.

The HREELS data do not provide much insight into the origin of the 420 K CO peak in the anisole/Pt(1 1 1) TPD data. We can speculate, however, to its origin. It is possible that cleavage of either C—O bond in adsorbed anisole may occur. As discussed above, $O—CH_3$ bond cleavage results in the formation of oxocyclohexadienyl as indicated by HREELS. In contrast, cleavage of the Ph—O (Ph = phenyl group) bond would produce an adsorbed phenyl group and an adsorbed methoxy group. At the temperature at which this reaction occurs it is likely that the methoxy group would rapidly decompose which could give rise to the 420 K desorption-limited CO peak. Decomposition of the phenyl group could contribute to the higher temperature H_2 desorption features. The reaction pathways for anisole on Pt(1 1 1) as determined from the TPD and HREELS data are summarized in Fig. 3.

3.2. Reaction of anisole on Zn/Pt(1 1 1)

Consistent with our previous studies of the reactivity of Zn-decorated Pt(1 1 1) surfaces [24,43], adding 0.2 ML of Zn adatoms to the Pt(1 1 1) surface significantly altered its reactivity toward anisole. TPD data obtained from 0.2 ML Zn/Pt(1 1 1) dosed with 0.6 L of anisole are displayed in Fig. 4. For this surface in addition to anisole, H_2 and CO, a range of other products were detected including CH_4, CH_2O, and C_2H_6. The low-temperature anisole desorption features were similar to those obtained from Zn-free Pt (1 1 1). Hydrogen primarily desorbed in two peaks centered at 450 and 500 K, and CO in a single peak at 500 K. Note that the large H_2 peak at 350 K for Pt(1 1 1) is nearly absent for Zn/Pt(1 1 1), and the onset of the primary H_2 and CO desorption features occurs at significantly higher temperatures (>100 K) on the Zn-modified surface. This indicates that Zn addition decreases the activity for C—H and C—C bond scission resulting in the adsorbed species derived from anisole being more stable on the Zn-modified surface. The observation of additional products from Zn/Pt(1 1 1) also indicates that the reactions on this surface are more selective. The CH_2O produced at 445 K likely results from cleavage of the Ph—O bond followed by dehydrogenation of the resulting methoxide group. Note that during methanol TPD on Zn/Pt(1 1 1), CH_2O is also produced near 445 K and previous studies have shown that this is a desorption-limited product [44]. Thus, in the case of anisole, Ph—O bond cleavage must occur below 445 K. Note that the Ph—O bond cleavage would also produce an adsorbed phenyl group and hydrogenation of this species could account for the small amount of benzene produced at 450 K.

HREEL spectra as a function of temperature for anisole-dosed Zn/Pt(1 1 1) are displayed in Fig. 5. As expected, at temperatures below 190 K the spectrum is nearly identical to that obtained in this temperature range for Zn-free Pt(1 1 1) and is consistent with IR and Raman spectra for anisole (see Table 1) [33–35]. Heating to 215 K, which is sufficient to desorb physisorbed anisole, caused some changes including the emergence of a small peak at 400 cm^{-1}, a large increase in the intensity of the $\delta(C—H)_{ring}$ peak at 1000 cm^{-1}, and a decrease in the intensities of the $\nu(C—H)$ peaks at 2880 and 3000 cm^{-1}. The peak at 400 cm^{-1} is at a position typically observed for metal–oxygen stretching modes [44–47]. In our previous study of the reaction of methanol on Zn/Pt(1 1 1), methoxide groups adsorbed on Zn sites also had a $\nu(Zn—O)$ stretch at this energy. This indicates that some adsorbed anisole binds to Zn sites on the surface via the oxygen.

Comparing the HREEL spectra for adsorbed anisole obtained near 200 K for both the Pt(1 1 1) and Zn/Pt(1 1 1) surfaces reveals that there is prominent peak at 1000 cm^{-1} in the spectrum from Zn/Pt(1 1 1) which is nearly absent in that from Pt(1 1 1). This peak is at the expected position for the in-plane $\delta(C—H)_{ring}$ mode of anisole. As discussed above, the absence of this in-plane mode in the Pt(1 1 1) spectrum at 200 K can be attributed to the aromatic ring being situated nearly parallel to the surface. In the case of Zn/Pt (1 1 1) the intensity of this peak indicates that the ring is tilted away from this surface. Note that this conclusion is consistent with what we have reported previously for the interaction of benzaldehyde with Pt(1 1 1) and Zn/Pt(1 1 1) surfaces [24]. Thus, based on

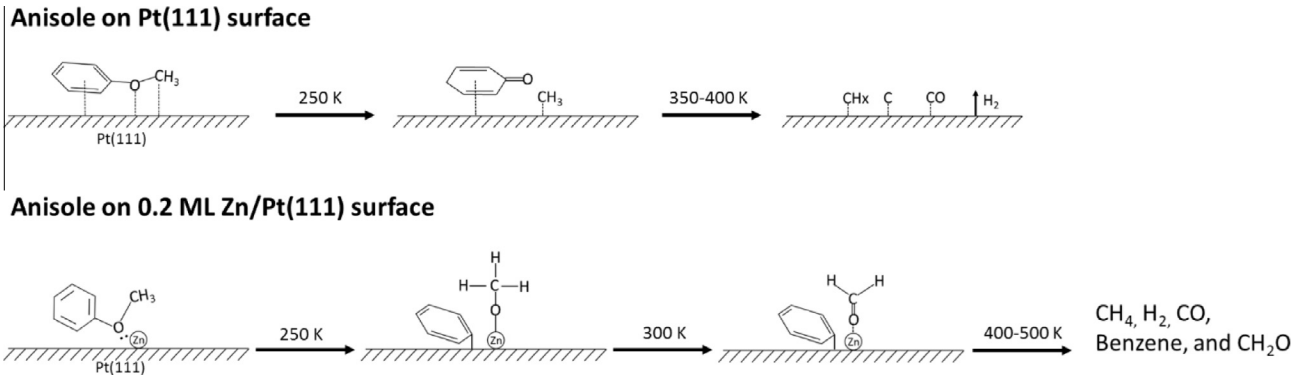

Fig. 3. Proposed pathways and intermediates for the adsorption and reaction of anisole on Pt(1 1 1) and Zn/Pt(1 1 1) surfaces.

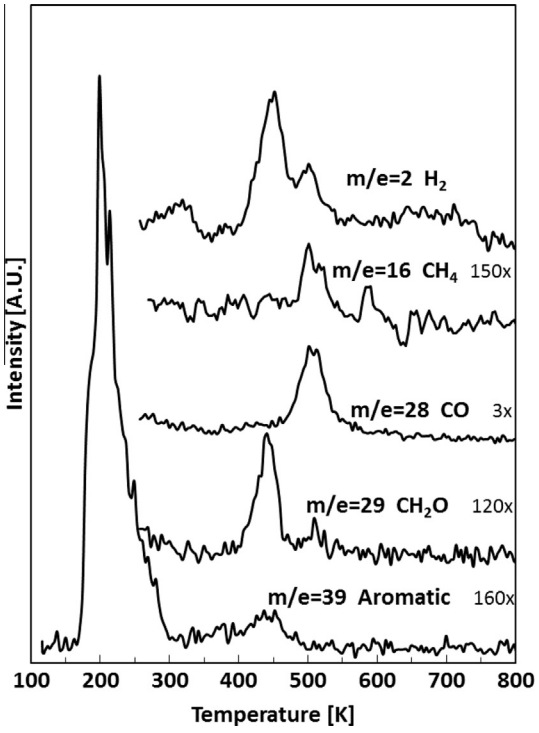

Fig. 4. TPD spectra obtained following exposure of the Zn/Pt(1 1 1) surface to 0.6 L of anisole.

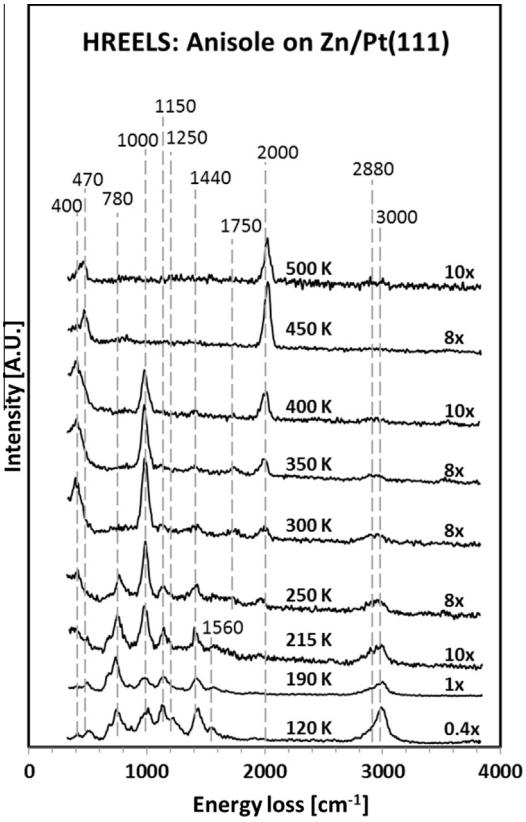

Fig. 5. HREEL spectra as a function of temperature for Zn/Pt(1 1 1) dosed with 0.6 L anisole at 115 K.

the HREELS data we propose that on Zn/Pt(1 1 1) anisole adsorbs via the oxygen as shown in Fig. 3, with the phenyl ring tilted away from the surface.

When the anisole-dosed Zn/Pt(1 1 1) surface was heated to 250 K, only minor changes occurred in the HREEL spectrum including further increases in the intensities of the peaks at 400 and 1000 cm^{-1} and a change in the relative intensities of the aliphatic and aromatic ν(C—H) peaks between 2800 and 3100 cm^{-1}. Also note that the high intensity of the peak at 1000 cm^{-1} relative to the other peaks suggests that modes in addition to the in-plane δ $(C—H)_{ring}$ mode of anisole contribute to this peak. Since C—O stretches of alkoxide groups are relatively intense and typically located near this energy [45–49], we propose that the ν(C—O) mode of methoxide groups formed via cleavage of the Ph—O bond in a portion of the adsorbed anisole contributes to the peak at 1000 cm^{-1}. This reaction would also produce an adsorbed phenyl group.

Heating the sample to 300 and then 350 K produced additional changes with the HREEL spectrum becoming dominated by the peaks at 400 and 1000 cm^{-1} and all the other peaks becoming less intense. A small ν(C—O) stretch at 2000 cm^{-1} also grows in which may be due in part to adsorption of some CO from the background. It is noteworthy that the spectrum at this temperature is nearly identical to that reported for methoxide groups adsorbed on this surface [44] which further supports the conclusion that C—O bond cleavage has occurred producing adsorbed methoxide. The persistence of the characteristic aromatic ν(C—H) peak at 3000 cm^{-1}, however, indicates that phenyl groups remain on the surface. At least a portion of these phenyl groups react to produce benzene that desorbs at 450 K as observed in the TPD data. Additional heating to 450 K resulted in the disappearance of the peaks associated with adsorbed hydrocarbon intermediates and the growth of the ν (C—O) stretch at 2000 cm^{-1} due to adsorbed CO.

The HREELS results for Zn/Pt(1 1 1) provide strong evidence for selective cleavage of the Ph—O bond in anisole to produce adsorbed methoxide and phenyl. While cleavage of the O—CH_3 bond in at least a portion of the absorbed anisole cannot be completely ruled out, the HREELS data do not provide any evidence for phenoxide or the oxocyclohexadienyl intermediate that was formed on the Zn-free Pt(1 1 1). As noted above, we have previously studied the reaction of CH_3OH on Zn/Pt(1 1 1) and in that study it was observed that methoxide groups formed by dissociative adsorption of methanol also reacted to form CH_2O which desorbed at 440 K [44]. XPS and HREELS results indicated that the methoxide groups involved in this reaction were adsorbed on Zn sites. Methanol TPD data as a function of Zn coverage also showed that the area of the 440 K CH_2O peak went through a maximum near 0.4 ML of Zn and disappeared for Zn coverages greater than 0.8 ML indicating that the initial dissociative adsorption of CH_3OH does not occur directly on the Zn sites, but rather on adjacent Pt sites whose electronic properties are modified by Zn adatoms. As has been shown in several previous studies [22–24,43], Pt—Zn interactions decrease the activity of the Pt surface for C—C and C—H bond activation resulting in adsorbed oxygenate and hydrocarbon intermediates being more stable on Zn-modified Pt compared to Zn-free Pt. Based on these previous results for methanol, we propose a similar scenario for the adsorption and reaction of anisole on Zn/Pt(1 1 1) with the initial chemisorption at low temperature occurring primarily on Pt sites adjacent to Zn adatoms. Selective cleavage of the Ph—O bond in these adsorbed anisole molecules produces methoxide groups that are bonded to the Zn atoms and phenyl groups bonded to adjacent Pt sites. This reaction pathway is shown in Fig. 3.

It is somewhat more difficult to account for the CO, CH_4 and H_2 products that desorb at 500 K from the anisole-dosed Zn/Pt(1 1 1) surface. The fact that these products are all produced at the same temperature indicates that they are reaction-limited and result from the decomposition of a common intermediate. While the HREELS data do not provide much insight into what this intermediate may be, it is possible that unselective decomposition of anisole occurs on non-Zn-modified portions of the surface producing adsorbed hydrocarbon fragments that undergo further decomposition near this temperature.

3.3. Reactor studies

The studies of the interaction of anisole with the model catalysts demonstrate that Zn addition to the Pt(1 1 1) surface affects reactivity in several ways, including altering the strength of the interaction of the phenyl ring with the surface, altering the barriers for C—H and C—C bond cleavage, and providing sites that are selective for C—O bond cleavage. On Zn-free Pt(1 1 1) there is a strong interaction between the phenyl ring and the surface resulting in a bonding geometry in which the ring is situated parallel to the surface. Anisole adsorbed in this configuration undergoes C—O and C—H bond scission at low temperatures to produce oxocyclohexadienyl and methyl groups with the former ultimately decomposing to produce CO, H_2 and small CH_x fragments. In contrast, on Zn-modified Pt(1 1 1) a different adsorption configuration and reaction pathway for anisole were observed. As has been reported previously in our benzaldehyde study [24], through an electronic interaction the Zn decreases the adsorption energy of the phenyl ring with the surface. This causes the preferred adsorption geometry to be one in which the phenyl ring is tilted away from the surface with bonding occurring primarily via the oxygen. Selective C—O bond scission in this species at or near Zn sites produces adsorbed phenyl groups and methoxide groups with the latter being bonded to the Zn sites. While cleavage of the O—CH_3 bond to produce phenoxide groups might also occur, the TPD and HREELS results did not provide direct evidence for this pathway. These reaction pathways are summarized in Fig. 3.

Based on the results obtained from the model catalysts one can speculate as to how the reactivity of supported Pt and Pt—Zn catalysts may differ for the HDO of anisole. Since the reaction of anisole on Pt(1 1 1) was not found to be selective for C—O bond cleavage, one would not expect high surface area Pt catalysts to be particularly selective for the reaction of anisole to produce benzene or phenol. The adsorption configuration of anisole on Pt(1 1 1) in which the phenyl ring lays flat on the surface may also help facilitate hydrogenation of the ring under typical HDO reaction conditions where there is a high partial pressure of H_2. Thus, one might also expect Pt catalysts to produce ring hydrogenation products for these conditions which are generally undesired since aromatic compounds have higher values. Since modifying Pt(1 1 1) with Zn changes the bonding configuration of anisole to one in which the primary interaction is via the oxygen with the phenyl ring tilted away from the surface, one would expect Pt—Zn catalysts to be less likely to promote ring hydrogenation under HDO conditions. The results obtained from Zn/Pt(1 1 1) also indicate that Zn provides sites that are selective for C—O bond cleavage as evidenced by the production of methoxide, as determined by HREELS, and benzene which was observed as product during TPD. These observations along with the fact that Zn addition appears to lower the activity of the Pt surface for C—C bond cleavage [22,24,43], suggest that high surface area Pt—Zn catalysts have some promise for the HDO of lignin-derived oxygenates to produce aromatic compounds.

In order to verify these predictions from the model catalyst results, we evaluated the performance of carbon-supported Pt and Pt—Zn catalysts for HDO of anisole using a tubular flow reactor. Details of the catalyst synthesis and reactor configuration are given in the experimental section. Conversion and product distributions for Pt/C and PtZn/C catalysts at a reaction temperature of 598 K are shown in Fig. 6. Note that only the condensable products were collected and analyzed and no ring opening products were detected. Also note that in addition to the products listed, some methane was likely produced.

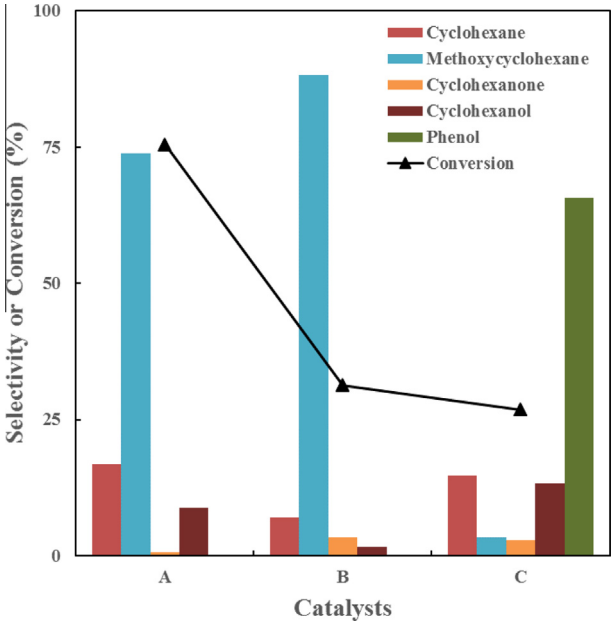

Fig. 6. Product distribution for reaction of anisole on different catalysts under typical HDO conditions: (A) 10 wt% Pt/C, W/F = 0.5 g min/ml, (B) 1 wt% Pt/C, W/F = 0.1667 g min/ml, (C) 10 wt% PtZn/C, W/F = 0.5 g min/ml, at 598 K and 27.5 bar.

As shown in Fig. 6, at a space time of 0.5 g min ml^{-1} the anisole conversion over 10 wt% Pt/C was 75% with a high selectivity to methoxycyclohexane which made up 74% of the condensable product. Smaller amounts of demethylation products, cyclohexane and cyclohexanol, were also produced. In order to determine the product selectivity at lower conversion (i.e. closer to differential reaction conditions) and to determine whether any other intermediate products were produced, experiments were also performed for a 1 wt% Pt/C catalyst with a reactant space time of 0.17 g min ml^{-1}. For these conditions the anisole conversion was only 31% but the selectivity to methoxycyclohexane increased to 88% and only small amounts of demethylation products, cyclohexane, cyclohexanone, and cyclohexanol, were produced. Using these data and an average Pt particle size as determined by TEM, the turnover frequency (TOF) for these reaction conditions is estimated to be 0.22 s^{-1}. This value is similar to that reported previously, 0.104 s^{-1}, for the gas phase HDO of anisole over a Pt/SiO_2 catalyst [25]. The increase in methoxycyclohexane selectivity with decreasing space time at the expense of the products requiring demethylation suggests that demethylation occurs after ring hydrogenation. Thus, on the Pt/C catalyst hydrogenation of the phenyl ring appears to be rather facile. This observation is consistent with the model catalyst studies which demonstrated an adsorption configuration for anisole on Pt(1 1 1) that would facilitate its hydrogenation, namely bonding via the π-orbitals of the phenyl ring with the ring lying flat on the surface. Thus, as predicted by the model catalyst studies, Pt/C has high activity for ring hydrogenation and low activity for selective C—O bond scission.

The conversion and product selectivity data for the 10 wt% PtZn/C catalyst at a reactant space time of 0.5 g min ml^{-1} are also presented in Fig. 6. These data show that, as expected, alloying Pt with Zn significantly alters reactivity. The PtZn/C catalyst has lower overall activity with the anisole conversion being less than half of that obtained for Pt/C at similar reaction conditions (corresponding to a TOF of 0.013 s^{-1} which was estimated assuming the same average particle size as the Pt/C catalyst). The PtZn/C catalyst is also highly selective for the production of phenol which represented 66% of the condensable product. Products requiring phenyl ring hydrogenation were also produced, most notably cyclohexane and cyclohexanol, but accounted for only ~27% of the condensable products.

It is likely that the co-impregnation method used to synthesize the Pt—Zn catalyst would produce metal particles with a range of Pt:Zn ratios. Since the Pt/C catalyst was highly active for phenyl ring hydrogenation it is possible that for the PtZn/C catalyst the ring hydrogenation products were produced on Pt-rich particles. To investigate this possibility and to assess the effect of Zn content on reactivity, reactor studies were also performed for a 10 wt% $PtZn_3/C$ catalyst which had a Pt:Zn ratio of 1:3. Conversion and product selectivity data as a function of reaction temperature for this catalyst are presented in Fig. 7 (W/F = 0.5 g min ml^{-1}, $P(H_2)$ = 27.5 bar). These data show that increasing the Zn content dramatically decreased overall activity with only 10% conversion at 598 K, but increased the selectivity to phenol to nearly 91%. Increasing the temperature to 623 and 648 K resulted in an increase in conversion but the high selectivity to phenol was maintained. These results support the possibility that in the case of the Pt—Zn catalyst the ring hydrogenation products were produced on Pt-rich particles.

It is important to note that while selective C—O bond scission was observed for both the model and high surface area PtZn catalysts, a different C—O bond was cleaved in each case. On Zn/Pt (1 1 1) cleavage of the Ph—O bond resulted in the production of benzene, while PtZn/C was selective for the less-desirable cleavage of the O—CH_3 bond leading to the production of phenol. The origin of this discrepancy is not clear, but the disparate reaction conditions between the UHV and reactor studies, *i.e.* the presence of a solvent (*n*-heptane) and a high pressure of H_2 in the case of the reactor studies, may have played a role. The surface structures of the model and high surface area catalysts are also likely to be much different. Nonetheless, it is interesting that in both cases the addition of Zn increases the selectivity for C—O bond cleavage and based on the model catalyst studies this appears to be due to surface Zn atoms providing a binding site for the oxygen in the anisole reactant.

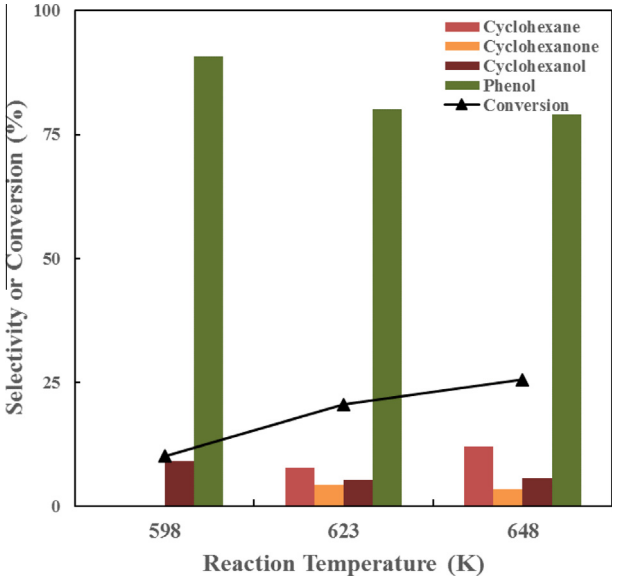

Fig. 7. Product distribution for reaction of anisole on $PtZn_3/C$ catalyst as a function of temperature. W/F = 0.5 g min/ml, 27.5 bar.

4. Summary

The combined surface science and reactor studies provide considerable insight into both the reactivity of aromatic oxygenates on Pt and how alloying with a second more oxyphilic metal, such as Zn, can be used to alter the reactivity and increase the selectivity for C—O bond cleavage which is required for HDO of this class of molecules. As described in the introduction, previous studies have suggested that alloying Pt with a more oxyphilic metal decreases the strength of the interaction of aromatic rings with the Pt surface [19–21]. The results obtained here show this quite dramatically for anisole where binding on Pt(1 1 1) occurs primarily via the π-orbitals of the phenyl ring with the ring situated parallel to the surface, while on Zn-modified Pt(1 1 1) the ring is tilted away from the surface and bonding occurs primarily via the oxygen lone pair electrons on a surface Zn site or possibly an adjacent Pt site. The reactor studies show that this difference in bonding geometry and adsorption sites has a significant effect on reaction selectivity. In particular the bonding geometry on Pt facilitates hydrogenation of the phenyl ring and the Pt/C catalyst exhibited high selectivity to saturated products, such as methoxycyclohexane and cyclohexane. In contrast on PtZn catalysts for which the model catalyst studies suggested that the phenyl ring will have limited interaction with the surface, ring hydrogenation was greatly suppressed with the primary reaction product being phenol.

The alteration of the interaction of the aromatic rings with the Pt surface appears to be largely an electronic effect of alloying with Zn. The results obtained here and in our previous studies [22–24,43], however, also show that the oxyphilic nature of the Zn makes it the preferred binding site for oxygen and an active site for selective C—O bond cleavage. This was shown for the Zn/Pt

(1 1 1) model catalyst where Zn-bound methoxide was observed as a primary reaction intermediate and for the high surface area PtZn/C catalysts which exhibited high selectivity to phenol. Apart from the specific case of PtZn which was investigated here, we believe the results of this study are more generally applicable and help explain why a range of bimetallic catalysts composed of a group 10 metal and a second more oxyphilic metal, e.g. PdZn, PdFe, NiFe, and PtSn [15–18], exhibits promising characteristics as catalysts for the HDO of lignin-derived oxygenates to produce high-value aromatic compounds.

Acknowledgment

Funding for this study was provided by the National Science Foundation Grant No. CBET-1508048.

Appendix A. Supplementary material

Supplementary data associated with this article can be found, in the online version, at http://dx.doi.org/10.1016/j.jcat.2016.05.020.

References

[1] H. Wang, J. Male, Y. Wang, ACS Catal. 3 (2013) 1047–1070.
[2] J. Zakzeski, P.C. Bruijnincx, A.L. Jongerius, B.M. Weckhuysen, Chem. Rev. 110 (2010) 3552–3599.
[3] G.W. Huber, J.A. Dumesic, Catal. Today 111 (2006) 119–132.
[4] G.W. Huber, S. Iborra, A. Corma, Chem. Rev. 106 (2006) 4044–4098.
[5] P. Gallezot, Chem. Soc. Rev. 41 (2012) 1538–1558.
[6] M. Stöcker, Ang. Chem. Int. Ed. 47 (2008) 9200–9211.
[7] E. Adler, Wood Sci. Technol. 11 (1977) 169–218.
[8] D. Mohan, C.U. Pittman, P.H. Steele, Energy Fuels 20 (2006) 848–889.
[9] Q. Bu, H. Lei, A.H. Zacher, L. Wang, S. Ren, J. Liang, Y. Wei, Y. Liu, J. Tang, Q. Zhang, Bioresour. Technol. 124 (2012) 470–477.
[10] A. Centeno, E. Laurent, B. Delmon, J. Catal. 154 (1995) 288–298.
[11] T.-R. Viljava, R. Komulainen, A. Krause, Catal. Today 60 (2000) 83–92.
[12] H. Wan, R.V. Chaudhari, B. Subramaniam, Topics Catal. 55 (2012) 129–139.
[13] D. Poondi, M.A. Vannice, J. Catal. 161 (1996) 742–751.
[14] S.D. Lin, M.A. Vannice, J. Catal. 143 (1993) 539–553.
[15] M.Á. González-Borja, D.E. Resasco, Energy Fuels 25 (2011) 4155–4162.
[16] J. Sun, A.M. Karim, H. Zhang, L. Kovarik, X.S. Li, A.J. Hensley, J.-S. McEwen, Y. Wang, J. Catal. 306 (2013) 47–57.
[17] T.H. Parsell, B.C. Owen, I. Klein, T.M. Jarrell, C.L. Marcum, L.J. Haupert, L.M. Amundson, H.I. Kenttämaa, F. Ribeiro, J.T. Miller, Chem. Sci. 4 (2013) 806–813.
[18] S. Leng, X. Wang, X. He, L. Liu, Y.e. Liu, X. Zhong, G. Zhuang, J.-G. Wang, Catal. Commun. 41 (2013) 34–37.
[19] C. Xu, Y.L. Tsai, B.E. Koel, Phys. Chem. 98 (1994) 585–593.
[20] J. Breitbach, D. Franke, G. Hamm, C. Becker, K. Wandelt, Surf. Sci. 507 (2002) 18–22.
[21] G. Hamm, T. Schmidt, J. Breitbach, D. Franke, C. Becker, K. Wandelt, Surf. Sci. 562 (2004) 170–182.
[22] J.R. McManus, E. Martono, J.M. Vohs, ACS Catal. 3 (2013) 1739–1750.
[23] J.R. McManus, E. Martono, J.M. Vohs, Catal. Today 237 (2014) 157–165.
[24] D. Shi, J.M. Vohs, Surf. Sci. (2015).
[25] X. Zhu, L.L. Lobban, R.G. Mallinson, D.E. Resasco, J. Catal. 281 (2011) 21–29.
[26] K.L. Deutsch, B.H. Shanks, Appl. Catal. A 447 (2012) 144–150.
[27] D.J. Rensel, S. Rouvimov, M.E. Gin, J.C. Hicks, J. Catal. 305 (2013) 256–263.
[28] J.R. McManus, M. Salciccioli, W. Yu, D.G. Vlachos, J.G. Chen, J.M. Vohs, J. Phys. Chem. C 116 (2012) 18891–18898.
[29] J.R. McManus, J.M. Vohs, Surf. Sci. 630 (2014) 16–21.
[30] C.-S. Ho, E. Martono, S. Banerjee, J. Roszell, J. Vohs, B.E. Koel, J. Phys. Chem. A 117 (2013) 11684–11694.
[31] J. Luo, L. Arroyo-Ramírez, R.J. Gorte, D. Tzoulaki, D.G. Vlachos, AIChE J. 61 (2015) 590–597.
[32] R. McCabe, L. Schmidt, Surf. Sci. 65 (1977) 189–209.
[33] L. Hoffmann, S. Marquardt, A. Gemechu, H. Baumgärtel, Phys. Chem. Chem. Phys. 8 (2006) 2360–2377.
[34] D.M. Adams, A. Squire, J. Chem. Soc. Dalton Trans. (1974) 558–565.
[35] J. Bloino, M. Biczysko, O. Crescenzi, V. Barone, J. Chem. Phys. 128 (2008) 244105.
[36] N. Bonalumi, A. Vargas, D. Ferri, A. Baiker, J. Phys. Chem. B 110 (2006) 9956–9965.
[37] N. Bonalumi, A. Vargas, D. Ferri, T. Bürgi, T. Mallat, A. Baiker, J. Am. Chem. Soc. 127 (2005) 8467–8477.
[38] M. Saeys, M.-F. Reyniers, G.B. Marin, M. Neurock, J. Phys. Chem. B 106 (2002) 7489–7498.
[39] J. Bertolini, G. Dalmai-Imelik, J. Rousseau, Surf. Sci. 68 (1977) 539–546.
[40] S.H. Pang, A.M. Román, J.W. Medlin, J. Phys. Chem. C 116 (2012) 13654–13660.
[41] H. Ihm, J. White, J. Phys. Chem. B 104 (2000) 6202–6211.
[42] D.H. Fairbrother, X. Peng, R. Viswanathan, P. Stair, M. Trenary, J. Fan, Surf. Sci. 285 (1993) L455–L460.
[43] D. Shi, J.M. Vohs, ACS Catal. 5 (2015) 2177–2183.
[44] E. Martono, J.M. Vohs, J. Phys. Chem. C 117 (2013) 6692–6701.
[45] K. Christmann, J. Demuth, J. Chem. Phys. 76 (1982) 6308–6317.
[46] B.A. Sexton, Surf. Sci. 102 (1981) 271–281.
[47] O. Skoplyak, C.A. Menning, M.A. Barteau, J.G. Chen, J. Chem. Phys. 127 (2007) 114707.
[48] C. Houtman, M.A. Barteau, Langmuir 6 (1990) 1558–1566.
[49] S.R. Bare, J.A. Stroscio, W. Ho, Surf. Sci. 150 (1985) 399–418.